Acta Geochim (2016) 35(4):391–407
DOI 10.1007/s11631-016-0124-4

ORIGINAL ARTICLE

The genetic relationship between Habo alkaline intrusion and its surrounding deposits, Yunnan Province, China: geological and S–Pb isotopic evidences

Zhongneng Meng[1,2] · Qian Zhang[1] · Lin Ye[1] · Yupin Liu[1] · Jiangbo Lan[1] · Dapeng Wang[1]

Received: 27 May 2016 / Revised: 4 August 2016 / Accepted: 6 September 2016 / Published online: 22 September 2016

Abstract The Habo alkaline intrusion, which is located in the south of the Sanjiang area, Yunnan Province, China, is a typical Cenozoic alkaline intrusion. There are a series of small to medium-sized Au and Pb–(Zn) deposits around this intrusion. Those deposits are spatially associated with the Habo alkaline intrusion. (1) The $\delta^{34}S$ values of sulfides from Au deposits range from −1.91 ‰ to 2.69 ‰, which are similar to those of Pb–(Zn) deposits (−3.82 ‰ to −0.05 ‰) and both indicate a much greater contribution from magma. (2) The Habo alkaline intrusion has relatively homogeneous Pb isotopic compositions with $^{206}Pb/^{204}Pb$ ranging from 18.608 to 18.761, $^{207}Pb/^{204}Pb$ from 15.572 to 15.722 and $^{208}Pb/^{204}Pb$ from 38.599 to 39.110. These Pb isotope ratios are similar to those of Au deposits, whose $^{206}Pb/^{204}Pb$ range from 18.564 to 18.734, $^{207}Pb/^{204}Pb$ from 15.582 to 15.738 and $^{208}Pb/^{204}Pb$ from 38.592 to 39.319. Pb ratios in both the intrusion and Au *deposits* suggest that Pb mainly derived from the depth, probably represents a mixture of mantle and crust. Pb–(Zn) deposits, however, show a decentralized trait, and most of them are similar to that of the alkaline intrusion with $^{206}Pb/^{204}Pb$ ranging from 18.523 to 18.648, $^{207}Pb/^{204}Pb$ from 15.599 to 15.802, and $^{208}Pb/^{204}Pb$ from 38.659 to 39.206. (3) In the plumbotectonic diagram $^{207}Pb/^{204}Pb$ versus $^{206}Pb/^{204}Pb$, almost all of Au and Pb–(Zn) deposits have the same projection area with the Habo alkaline intrusion, which indicates that those deposits almost share the same source with the alkaline intrusion. (4) Isotopic age of the Habo alkaline intrusion is 36–33 Ma, which is similar to that of Beiya, whose ore-related alkaline porphyries age is 38–31 Ma and molybdenite Re–Os age is 36.9 Ma. Therefore, along with S–Pb isotope traits, we suggest that the Habo Au and Pb–(Zn) deposits should be typically Ailaoshan-Red RiverCenozoicalkaline-related deposits and ore-forming ages of these deposits should be later than that of the Habo alkaline intrusion.

Keywords The Habo Au and Pb–(Zn) deposits · Alkaline intrusion · Ore genesis · S–Pb isotope analyses · Source materials

1 Introduction

As a typical alkaline intrusion in the south of the Ailaoshan-Red River alkaline intrusion belt (Bi et al. 2005), the Habo alkaline intrusion has gradually become a research focus recently (Zhu et al. 2009, 2013; Zhao et al. 2009). Meanwhile, a series of porphyry deposits (such as the Habo Cu–Mo deposit), fracture hydrothermal vein type Au deposits (such as the Habo Au deposit, the Hageng Au deposit, and the Shapu Au deposit), and fracture hydrothermal vein type deposits [such as Shee Pb–(Zn) deposit, Adong Pb–(Zn) deposit, and Duojiao Pb–(Zn) deposit], which are spatially associated with the Habo alkaline intrusion, have begun to attract the attention of scholars. Zhu et al. (2013) suggested that the formation of the Habo Cu–Mo deposit should be a continuous process that occurred as a response to regional tectonic movements. The Habo deposit may also represent the southeasterly extension of the Yulong porphyry metallogenic belt. Zhao

✉ Qian Zhang
zhangqian@vip.gyig.ac.cn

[1] State Key Laboratory of Ore Deposit Geochemistry, Institute of Geochemistry, Chinese Academy of Sciences, Guiyang 550081, China

[2] University of Chinese Academy of Sciences, Beijing 100049, China

et al. (2009) suggested that the genesis of the Habo Au deposit belong to volcanic sedimentary hydrothermal reformation type deposit. This conclusion, however, needs more reliable geochemistry evidence. Studies on other Au deposits and Pb–(Zn) deposits, however, are extremely weak. Therefore, the origin and genetic relationship between Habo alkaline intrusion and Au and Pb–(Zn) deposits are still unclear and worth studying.

A lot of research show that S–Pb isotopes can effectively trace the source of the metal elements within the metallogenic system (Ohmoto 1972; Rey and sawkins 1974; Ohmoto et al. 1990; Zheng and Hoefs 1993; Seal 2006; Basuki et al. 2008; Zhou et al. 2010, 2013a, b, 2014, 2016). Based on the detailed description of the geological features of the Habo alkaline intrusion and the Habo Au and Pb–(Zn) deposits, this paper systematically studies Pb isotope compositions of this intrusion and S–Pb isotope compositions of those deposits to tackle the above academic issues.

2 Geological setting

2.1 Regional geology

Sanjiang area has suffered intense deformations caused by the collision between India and Asia continents since 65 Ma and a series of NW to NNW trending of strike-slip fault systems and fold belts are formed then. For instance, the Ailaoshan-Red River Fault Zone, the Chongshan Fault Zone and the Gaoligong-Shijie Fault Zone (Zhang et al. 1987, 2009; Turner et al. 1996; Chung et al. 1997; Wang and Burchfiel 1997; Ji et al. 2000; Yin and Harrison 2000; Hou et al. 2003). A belt of one-thousand km long, 50–80 km wide alkali-rich intrusive rocks (potassic igneous rocks) outcropped along with the formation of the Cenozoic strike-slip fault systems, which were controlled by the Cenozoic intracontinental strike-slip tectonic stress field (Hou et al. 2006) and then distributed around this fault systems, which were named Ailaoshan-Red River Alkali-rich Intrusive Rocks Belt (Bi et al. 2005). Recent studies have shown that those alkali-rich intrusive rocks have close relationship with the formation of gold, copper and molybdenum mines and have formed a number of porphyry metallogenic systems. For instance, the Narigongma porphyry copper–molybdenum deposit and the Yulong porphyry copper deposit located in the north of the rocks and the Beiya alkaline porphyry Au deposit and the Machangqing porphyry copper–molybdenum deposit is located in the south (Fig. 1), which has been called the Ailaoshan-Red River Cenozoic Ore System (Zhang and Xie 1997; Hu et al. 2004; Wang et al. 2001, 2004; Hou et al. 2003; Bi et al. 2005).

The Ailaoshan-Red River Fault Zone has suffered multi-phased sinistral strike-slip faulting since Cenozoic and, at the same time, led to the emplacement of several alkali-rich rocks. Most of those rocks occur as the shapes of rock stub and vein group, and they distribute on both sides of the Ailaoshan-Red River strike-slip fault system. These alkali-rich rocks are controlled by the secondary fracture of Ailaoshan-Red River strike-slip fault, and the main rock types are granite porphyry, quartz monzonite porphyry and quartz syenite porphyry. It has been considered that most of these porphyries have close relations with the mineralization of Au, Cu, Mo, Pb and Zn, which makes many Scholars begin to focus on those porphyry rocks. Alkali-rich rock groups that have been discovered till now are, according to their spatial distribution, Bengge-Jianchuan alkali-rich rock group, Ninglang-Yongsheng alkali-rich rock group, Beiya alkali-rich rock group, Yaoan alkali-rich rock group, Tongchang alkali-rich rock group and Habo alkali-rich rock group (Fig. 1).

The Habo alkaline intrusion, which belongs to Habo alkali-rich rock group, emplaced on the Oumei fault in a nearly SN direction with an area of 26.2 km^2 and is composed of four rock units. They are, by their respective emplacement orders, Pingshan unit (EP), Sandaoban unit (ES), Ashu unit (EA) and Habonanshan unit (EH) (Fig. 2). Our recent unpublished studies show that the constraints of these rock units are: (1) Pingshan unit distributed in south of Habo porphyry intrusion and it is mainly composed of biotite amphibole syenite, zircon grains of Pingshan biotite amphibole syenite yield a weighted mean $^{206}Pb/^{238}U$ age of 36.48 ± 0.45 Ma; (2) Sandaoban unit scattered in the intrusion and it is mainly composed of altered biotite amphibole syenite, zircon grains of Sandaoban altered biotite amphibole syenite yield a weighted mean $^{206}Pb/^{238}U$ age of 35.41 ± 0.34 Ma; (3) Ashu unit is the largest one that outcropped in the Habo alkaline intrusion. Its chief rock type is biotite pyroxene syenite, zircon grains of Ashu biotite pyroxene syenite yield a weighted mean $^{206}Pb/^{238}U$ age of 36.88 ± 0.65 Ma; (4) Habonanshan unit exposed in the centre of Ashu unit, and the chief rock types of this area are pyroxene syenite and quarts amphibole syenite, zircon grains of Habonanshan rocks yield a weighted mean $^{206}Pb/^{238}U$ age of 33.53 ± 0.35 Ma, which is consistent with previous studies (Zhu et al. 2013). This intrusion is in uncomfortable contact with the middle Waimaidi formation of Paleozoic Madeng rock groups, Silurian and Triassic formations. Detailed descriptions of these formations are given in Table 1. The Paleozoic Madeng rock group, which is of extraordinary importance in this area, mainly consists of metamorphic rocks and has been divided into two formations, namely Waimaidi formation and Qihaiyan formation, and, at the same time, they are in comfortable contact with each other. The Waimaidi

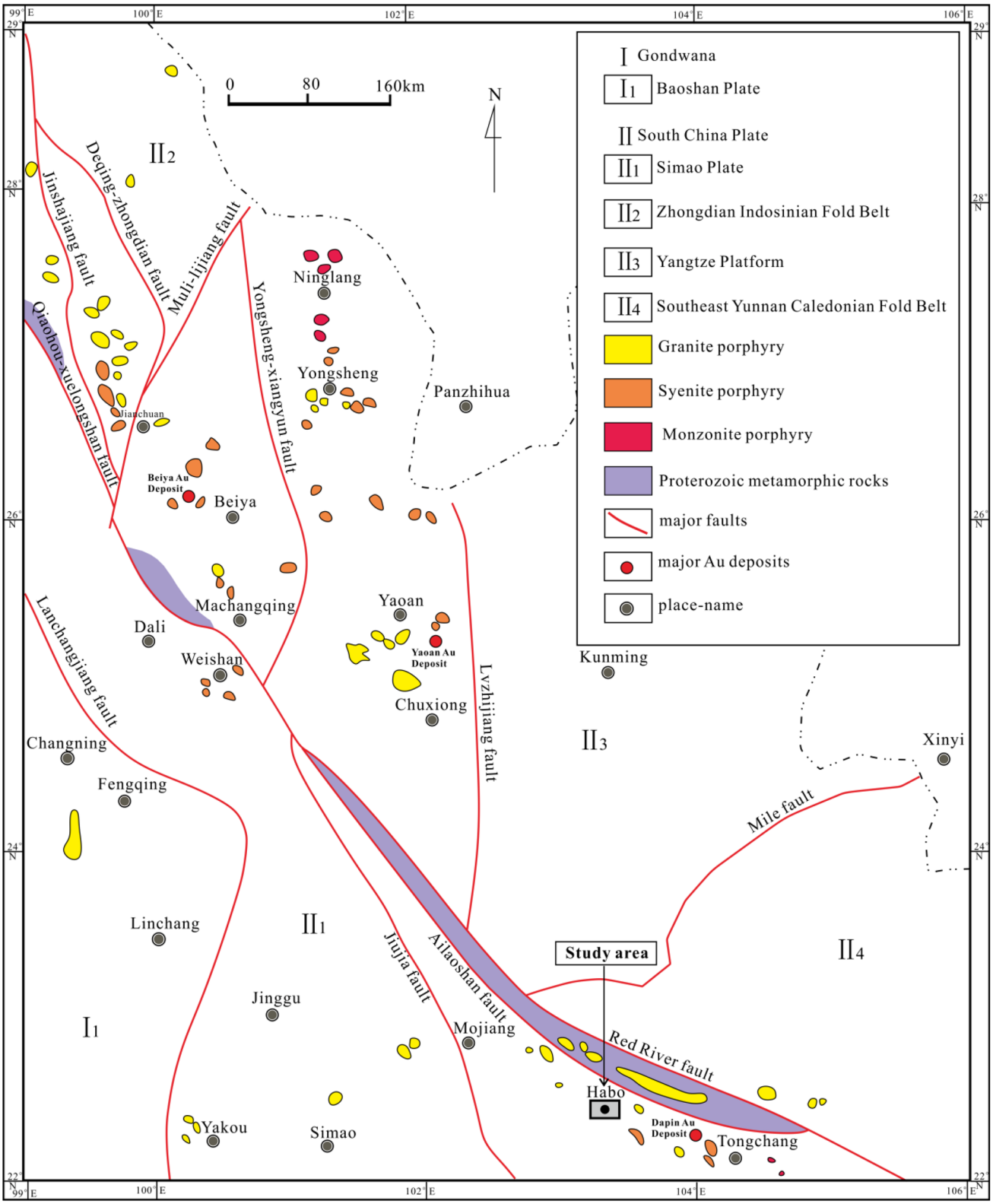

Fig. 1 Distributions of Cenozoic alkaline rocks and related Au deposits in the western Yunnan Province

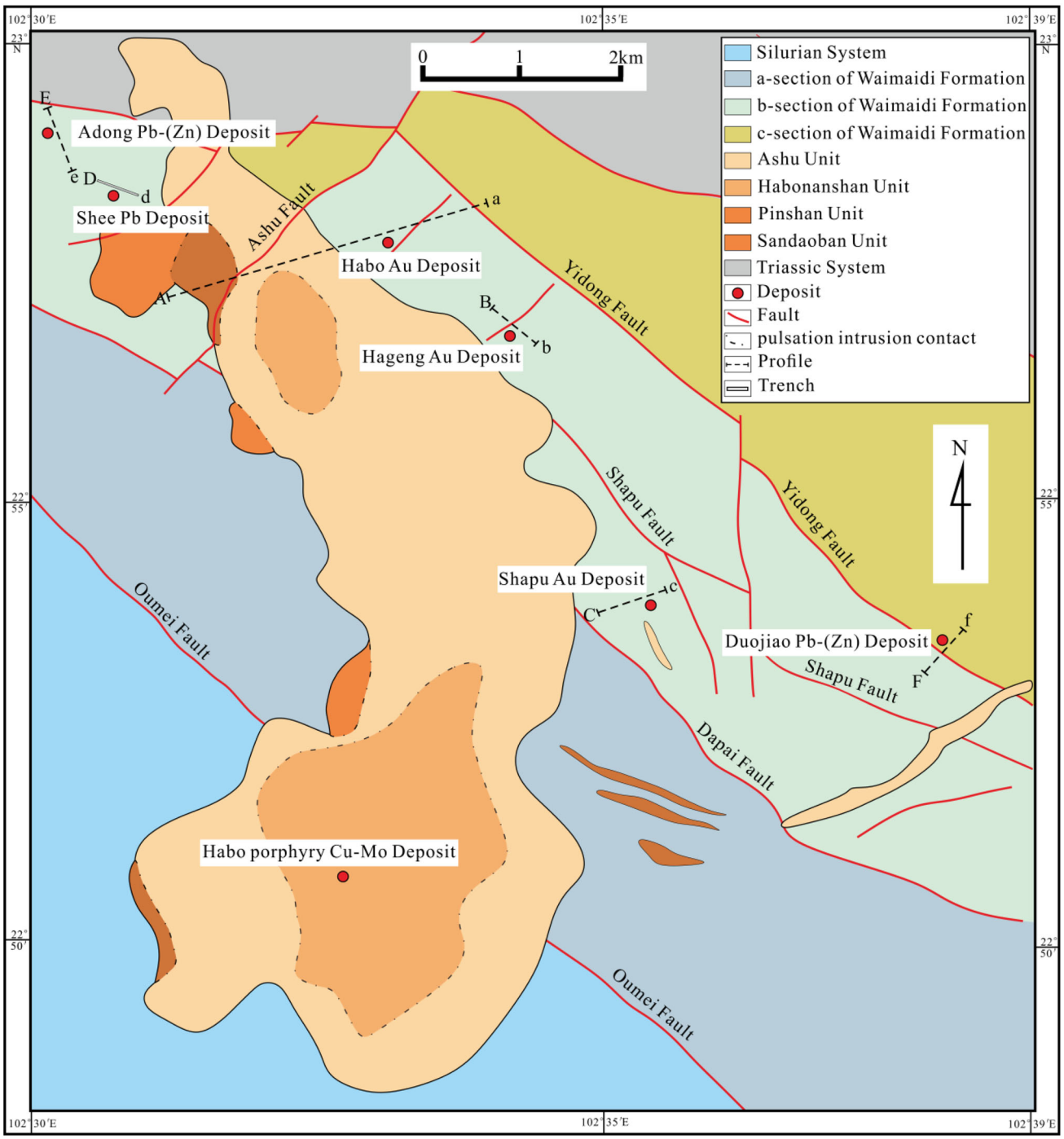

Fig. 2 Distributions of Habo four rock units and Cu–Mo, Au and Pb–(Zn) deposits around the Habo alkaline intrusion. (Redrawn after Yunnan No. 2 Geological Survey)

formation consists of three layers, including, from west to northeast, a, b, and c-section Waimaidi formation and they are in comfortable contact with each other.

The Habo Cu–Mo, Au and Pb–(Zn) deposits are situated in the south of the Ailaoshan-Red River Cenozoic Ore System and are located between the Red River Fault and the Jiujia Fault. Fractures in this study area are a series of NW trending faults and cut by NE trending secondary faults (Fig. 2). Major faults in this study area are the Oumei Fault, the Dapai Fault, the Shapu Fault, the Yidong Fault and the Huangchaoling Fault. Deposits in this area are spatially associated with the Habo alkaline intrusion (Fig. 2). Among them, (1) the Habo porphyry Cu–Mo deposit is hosted by the Habo granite pluton,

Table 1 Characteristic of stratums distributed around the Habo alkaline intrusion

Geological age	Formation	Thickness	Lithological description
Triassic	Waigucun formation (T_3W)	More than 900 m	Slate, dark gray crystalline limestone, grey sandstone, quartz sandstone, sandstone, conglomerate
Paleozoic	c-section Waimaidi formation (P_zw^c)	Unknown	Gray sericite quartz phyllite, dark gray sericite phyllite, chlorite quartz phyllite chlorite sericite quartz phyllite
	b-section Waimaidi formation (P_zw^b)		Py-forming limestone, banded siliceous rock, sericite quartz phyllite, banded sericite phyllite, quartz phyllite, quartz sandstone, phyllitic slate, quasi-mylonite
	a-section Waimaidi formation (P_zw^a)		Gray sericite phyllite, meta-quartz sandstone, quartz sandstone, quartz phyllite, quasi-mylonite
Silurian	Manpo formation ($S_{2\text{-}3}m$)	More than 1719 m	Gray meta-quartz sandstone, meta-siltstone, metamorphic feldspar quartz- sandstone, silty slate, crystalline limestone

which was emplaced into Paleozoic and Silurian metamorphic rocks (Zhu et al. 2009), and its ore-controlling structures are secondary faults of the Oumei Fault (this deposit is not the focus of this paper); (2) the Habo Au deposit occurs at the north exocontact of the Habo alkaline intrusion. Its wall rock is the b-section Waimaidi formation of Paleozoic Madeng rock groups and the ore bodies are controlled by the secondary faults of the Yidong Fault; (3) the Hageng Au deposit is situated in east 2 km of the Habo Au deposit and occurs at the NE margin of the alkaline intrusion. And the host rock of this deposit is the b-section Waimaidi formation and its ore-controlling fractures are secondary faults of the Yidong Fault; (4) the Shapu Au deposit is located in the east margin of the exocontact of the intrusion, and the wall rock of this deposit is the b-section Waimaidi formation and its ore-controlling fractures are secondary faults of the Shapu Fault; (5) the Shee Pb deposit occurs at the north exocontact of the Habo Habo alkaline intrusion. Its wall rock is the b-section Waimaidi formation and the ore bodies are controlled by a series of NE trending secondary faults; (6) the Adong Pb–(Zn) deposit occurs at the northwest of the Habo alkaline intrusion. Its wall rock is the b-section Waimaidi formationand the ore bodies are controlled by a series of NE-SW trending secondary faults; (7) the Duojiao Pb–(Zn) deposit occurs at the east of the Habo alkaline intrusion. Its wall rock is the c-section Waimaidi formation of Paleozoic Madeng rock groups and its ore bodies are controlled by a series of NE-SW trending secondary faults of the Yidong Fault.

2.2 Ore deposit geology of Au and Pb–(Zn) deposits

Au and Pb–(Zn) deposits are all distributed around the Habo alkaline intrusion. Rocks exposed are a, b sections Waimaidi formation. Detailed deposits descriptions are given in Table 2.

2.2.1 Au deposits

The three studied Au deposits, Habo, Hageng and Shapu, are fracture hydrothermal vein type deposits and are located within the b-section of the Waimaidi formation. Those deposits share several similar characteristics. They are positioned close to the Habo alkaline intrusion, which is about 1 km to the S in the case of Habo, 1 km to the W of Hageng, and 2 km to the W of Shapu (Fig. 2). The ore-bearing rocks are composed of Py-forming limestone, banded siliceous rock, sericite quartz phyllite, banded sericite phyllite, quartz phyllite, quartz sandstone, phyllitic slate and quasi-mylonite. In general, the ore bodies occur as bedded, veined and lenticular (Figs. 3 and 4), and all are faults controlled. Among them, (1) the thickness of ore bodies of Habo ranges from 2.51 to 3.99 m, with lengths varying from 52 to 600 m, and relatively steep dip (Fig. 3a). Ore minerals in ores are pyrite, limonite, sphalerite, galena, arsenopyrite, chalcopyrite and malachite (Fig. 4a–c). Gangue minerals in ores are quartz and sericite, followed by chlorite and feldspar. Among the metal minerals, pyrite occur in forms of both panidiomorphic–hypidiomorphic cubic and anhedral crystal aggregations and the size ranges from 0.1 to 0.5 mm. The cubic pyrite appears as spots or disseminations. The anhedral pyrite, however, appears as veinlets or masses, spots and dissemination. Sphalerite and galena occur as non-panidiomorphic crystals with tiny sizes and appear as veinlets (Fig. 4b, c). According to the field and laboratory identification, it can be concluded that the minerals sequences maybe are: pyrite (main Au-forming mineral)—arsenopyrite–chalcopyrite–sphalerite–galena–limonite. (2) The thickness of ore bodies of Hageng ranges from 0.25 to 1.00 m, with lengths varying from 30 to 50 m, and relatively steep dip (Fig. 3b). Major ore minerals is pyrite (Fig. 4e), followed by chalcopyrite, limonite and galena (Fig. 4f). Gangue minerals are quartz and

Table 2 Geological characteristics of the Au and Pb–(Zn) deposits distributed around the Habo alkaline intrusion

Deposit name and latitude	Ore-hosting stratum	Composition and thickness of the ore-bearing rock series	Ore body morphology and grade of metal	Mineral association within theore body	Ore texture and structure	Ore controlling structures
Habo Au deposit 22°55′3″N 102°35′49″E	b-section Waimaidi formation	The ore-bearing rock is composed of Py-forming limestone, banded siliceous rock, sericite quartz phyllite, banded sericite phyllite, quartz phyllite, quartz sandstone, phyllitic slate and quasi-mylonite	A total of 3 ore bodies are bedded, veined and lenticular. Strike NW–SE, dip direction SW, dip angle 26° to 81°, length 52–600 m, thickness 2.51–3.99 m. Au 3.18–3.38 g/t, average 3.28 g/t[a]	Ore minerals: pyrite, limonite, sphalerite, galena, chalcopyrite and arsenopyrite Gangue minerals: quartz, sericite, chlorite and feldspar	Panidiomorphic, hypidiomorphic and anhedral texture Massive, dissemvxinated, spots and veinlet structure	Ore bodies are controlled by the NWW-trending fault, which is the secondary faults of Yidong fault
Hageng Au deposit 22°54′15″N 102°36′51″E	b-section Waimaidi formation	The ore-bearing rock is composed of Py-forming limestone, banded siliceous rock, sericite quartz phyllite, banded sericite phyllite, quartz phyllite, quartz sandstone, phyllitic slate and quasi-mylonite	A total of 2 ore bodies occur as veined shape strike NW–SE, length 30–50 m, thickness 0.25–1.00 m, TFe 25 %–45 %[a], Au 0.10–23.70 g/t[a]	Ore minerals: pyrite, limonite, sphalerite, galena and chalcopyrite Gangue mineral: quartz	Panidiomorphic, hypidiomorphic and anhedral texture Massive structure	Ore bodies are controlled by the secondary faults of NW-trending fault
Shapu Au deposit 22°52′19″N 102°37′12″E	b-section Waimaidi formation	The ore-bearing rock is composed of Py-forming limestone, banded siliceous rock, sericite quartz phyllite, banded sericite phyllite, quartz phyllite, quartz sandstone, phyllitic slate and quasi-mylonite	A total of 5 ore bodies occur as veined and lenticular. Strike NW–SE, length 55–168 m, average Au 1.44 g/t[b]	Ore minerals: pyrite, limonite Gangue mineral: quartz	Panidiomorphic, hypidiomorphic and anhedral texture. Massive and disseminated structure	Ore bodies are controlled by the secondary faults of Shapu fault
Shee Pb deposit 22°57′51″N 102°32′19″E	b-section Waimaidi formation	The ore-bearing rock is composed of Py-forming limestone, banded siliceous rock, sericite quartz phyllite, banded sericite phyllite, quartz phyllite, quartz sandstone, phyllitic slate and quasi-mylonite	The ore bodies occur as veined and lenticular. Strike NE–SW	Ore minerals: cerusite, anglesite, pyrite and limonite Gangue minerals: quartz and calcite	Panidiomorhic, hypidiomorphic and anhedral texture Disseminated and brecciated structure	Ore bodies are controlled by the NE-trending fault
Adong Pb–(Zn) deposit 22°58′47″N 102°30′40″E	b-section Waimaidi formation	The ore-bearing rock is composed of Py-forming limestone, banded siliceous rock, sericite quartz phyllite, banded sericite phyllite, quartz phyllite, quartz sandstone, phyllitic slate and quasi-mylonite	The ore bodies occur as veined or lenticular. Strike NE-SW, the largest ore body length 200 m, thickness 1.00–3.55 m, average 2.45 m, Pb 2.82 %, Zn 4.00 %[c]	Ore minerals: pyrite, sphalerite, galena and chalcopyrite Gangue minerals: quartz and calcite	Panidiomorphic, hypidiomorphic and anhedral texture Massive and vein structure	Ore bodies are controlled by the NE-trending faults, which are the secondary faults of Huang-chaoling fault
Duojiao Pb–(Zn) deposit 22°51′47″N 102°38′15″E	c-section Waimaidi formation	Gray sericite quartz phyllite, dark gray sericite phyllite, chlorite quartz phyllite chlorite sericite quartz phyllite	The ore bodies occur as veined or lenticular. Strike NW–SE	Ore minerals: sphalerite and galena Gangue minerals: quartz and calcite	Anhedral or spots texture. Vein and brecciated structure	Ore bodies are controlled by the NW–SE trending Yidong faults

[a] Yunnan No. 2 Geological survey

[b] Yuanyang Resources development company of Yunxi group (2014)

[c] Yunnan Special Geological Mining Engineering company (2004)

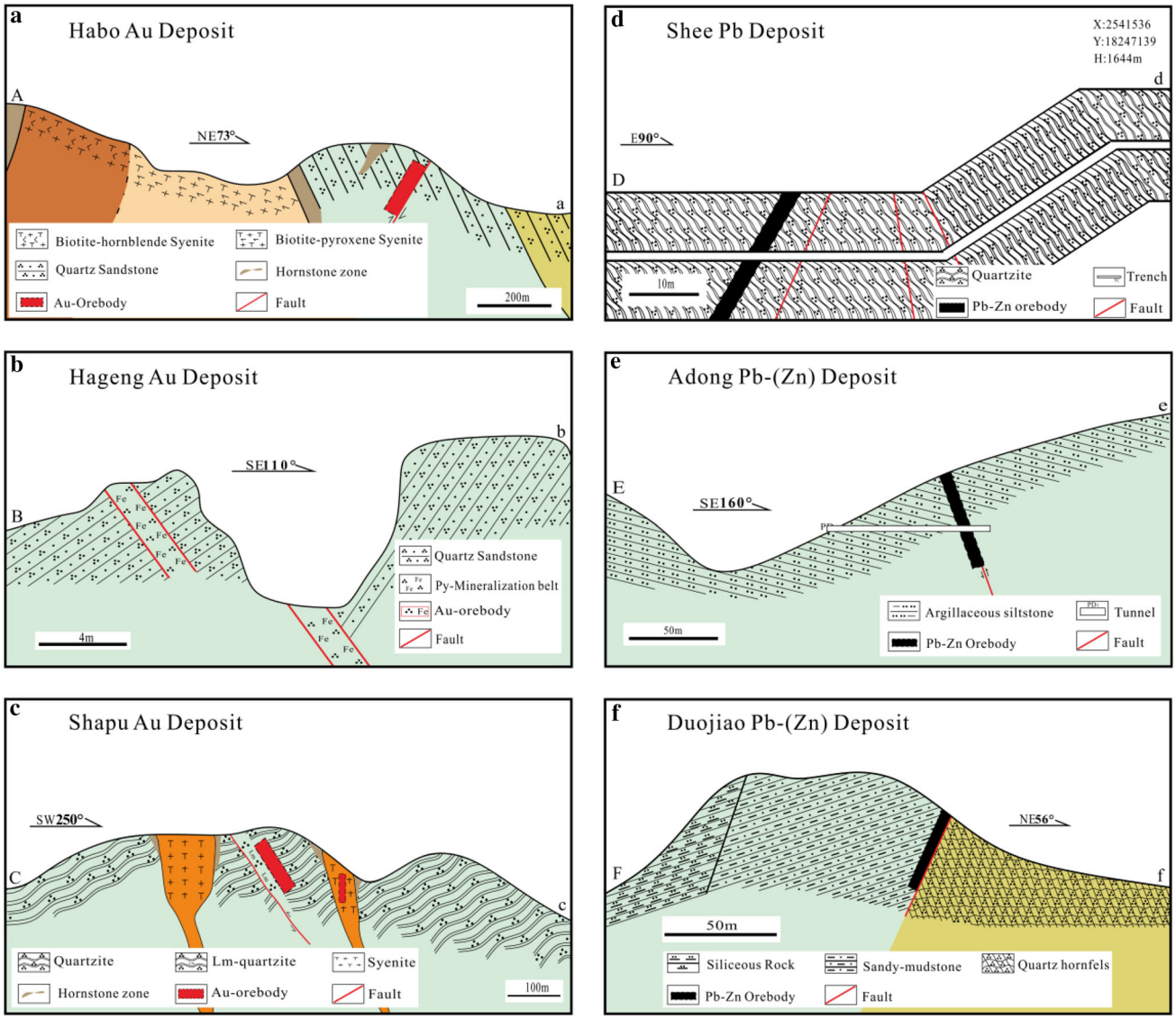

Fig. 3 Representative profiles through the Au and Pb–(Zn) deposits

sericite, followed by chlorite and feldspar. Among the ore minerals, pyrite occurs in form of bulky cubic crystals and distributes along in minerals. Chalcopyrite and galena appear as spots and distribute in the edge or gaps of pyrite or limonite. The minerals sequences maybe are: pyrite–chalcopyrite–galena–limonite. The wall-rock alterations that have deep relations with Au-mineralization mainly are silicification, pyritization, limonitization and sericitization. (3) The thickness of ore bodies of Shapu ranges from 1.5 to 10 m, with lengths varying from 55 to 168 m, and relatively steep dip (Fig. 3c). Major ore minerals is pyrite (Fig. 4d), followed by limonite. Gangue minerals are quartz and sericite, followed by chlorite and feldspar. The wall-rock alterations that have deep relations with Au-mineralization mainly are silicification, pyritization, limonitization and sericitization.

2.2.2 *Pb–(Zn) deposits*

The three studied Pb–(Zn) deposits, Shee, Adong and Duojiao, are fracture hydrothermal vein type deposits and are located within b and c-section of the Waimaidi formations. Those deposits share several similar characteristics. They are positioned distal to the Habo alkaline intrusion, which is about 2 km to the S in the case of Shee, 3 km to the S of Adong, and 4 km to the W of Duojiao (Fig. 2). The ore-bearing rocks are composed of Py-forming limestone, banded siliceous rock, sericite quartz phyllite, banded sericite phyllite, quartz phyllite, quartz sandstone, phyllitic slate and quasi-mylonite. In general, the ore bodies occur as bedded, veined and lenticular (Figs. 3 and 4), and all are faults controlled. Among those deposits, (1) The thickness of ore bodies of Shee ranges from 1.00 to 2.5 m, with lengths

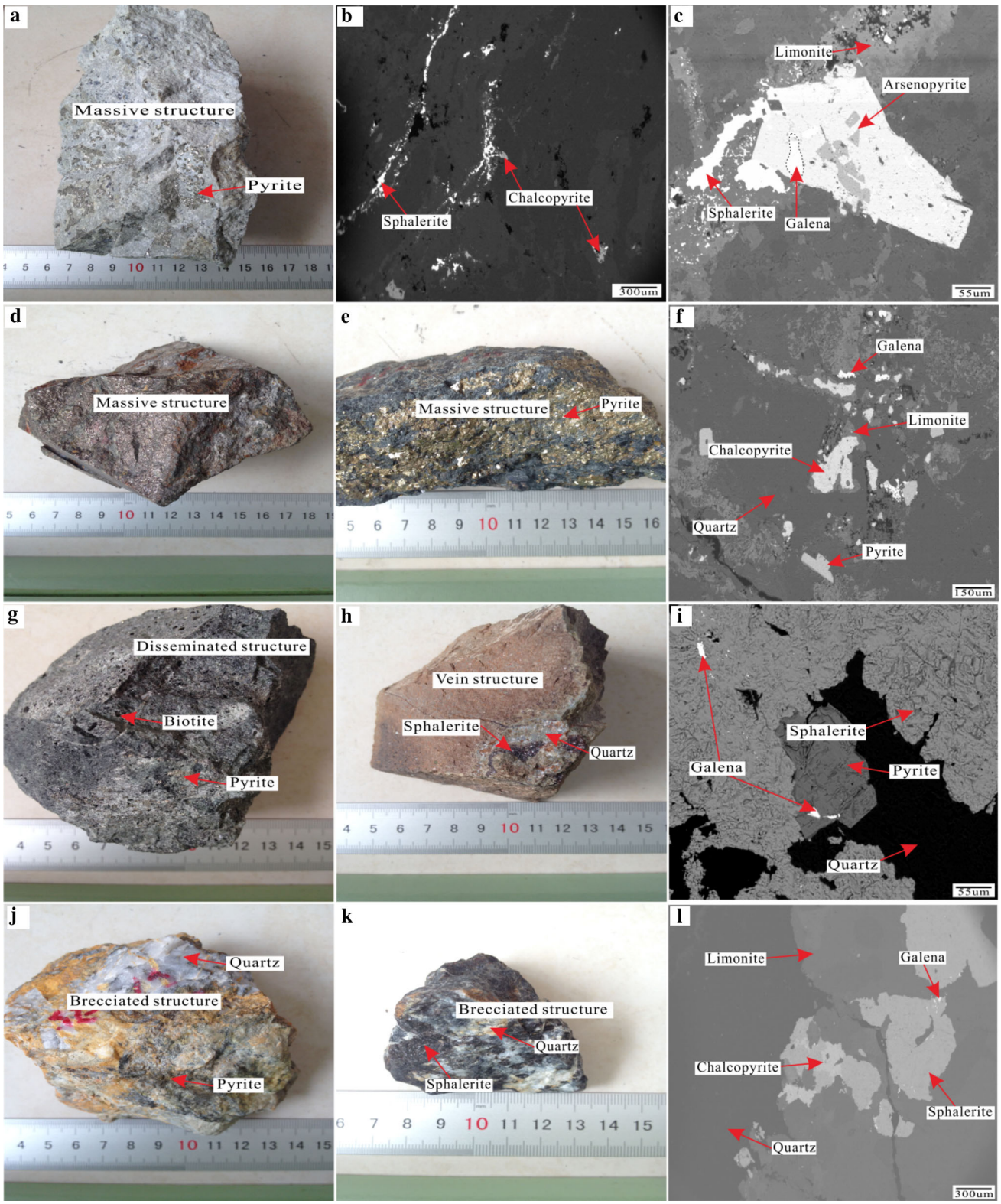

varying from 5 to 150 m, and relatively steep dip (Fig. 3d). Ore minerals of the Shee are cerusite, anglesite, hemimorphite, limonite, sphalerite, chalcopyrite and pyrite (Fig. 4g, j). Gangue minerals are calcite and quartz (Fig. 4j), followed by little barite and biotite. Among the gangue minerals, calcite occurs in the form of plate aggregation and often appears in the high-level mineralization areas as veins. Wall-rock alterations, for instance, silicification, pyritization,

◀**Fig. 4** Hand specimens and EPMA images from the studied deposits that distributed around the Habo alkaline intrusion. **a**, **b** and **c** are from the Habo Au deposit; **a** massive structure, major ore mineral is pyrite, **b** sphalerite aggregations and chalcopyrite spots, **c** replacement of sphalerite by limonite, replacement of galena by sphalerite, arsenopyrite enclosed by sphalerite, **d** is from Shapu Au deposit: massive sutructure, major ore mineral is pyrite, **e** is Hageng Au deposit: massive structure, major ore mineral is pyrite, **f** is from Hageng Au deposit: pyrite and galena spots, replacement of sphalerite by limonite, **g** is from Shee Pb deposit: disseminated structure, major ore mineral is pyrite, **h** is from Adong Pb–(Zn) deposit: vein structure, major ore mineral is sphalerite, major gangue mineral is quartz, **i** is from Adong Pb–(Zn) deposit: galena spots enclosed by sphalerite and pyrite, pyrite associated with sphalerite, **j** is from Shee Pb deposit: brecciated structure, major ore mineral is pyrite, major gangue mineral is quartz, **k** is from Duojiao Pb–(Zn) deposit: brecciated structure, major ore mineral is sphalerite, major gangue mineral is quartz, **l** is from Duojiao Pb–(Zn) deposit: sphalerite enclosed by limonite, replacement of chalcopyrite and galena by sphalerite

limonitization and carbonatization, are well-developed in the crushed zone. (2) The thickness of ore bodies of Adong ranges from 1.00 to 3.55 m, with lengths varying from 10 to 200 m, and relatively steep dip (Fig. 3e). Major ore mineral of this deposit is sphalerite (Fig. 4h), followed by galena and pyrite (Fig. 4i). Gangue minerals are calcite and quartz (Fig. 4h), followed by little barite. Among the gangue minerals, calcite occurs in the form of plate aggregation and often appears in the high-level mineralization areas as veins. Mineral phases and Electron probe analyses show that pyrite occurs as euhedral-big crystals and distributes among galena with spots. Chalcopyrite occurs in the cracks of quarts-veins as anhedral or distributes in galena and sphalerite as micro-inclusions. Galena and sphalerite often occur as anhedral and big crystals (0.1–1 mm). In conclusion, the minerals sequences maybe: pyrite-chalcopyrite-sphalerite-galena. (3) The thickness of ore bodies of Duojiao ranges from 1.00 to 2.00 m, with lengths varying from 5 to 40 m, and relatively steep dip (Fig. 3f). Ore minerals are sphalerite, galena, and limonite (Fig. 4k, l). Sphalerite is often associated with quartz (Fig. 4k). Gangue mineral is quartz (Fig. 4k). Mineral phases and Electron probe analyses show that the minerals sequences maybe: chalcopyrite–galena–sphalerite–limonite. Alterations, for instance, limonitization, silicification and quartzite, are widely distributed in the contact zone.

From geological descriptions above, it can be concluded that the ore-bearing rock series, morphology of ore bodies, and characteristics of ores are similar to those Au and Pb–(Zn) deposits.

3 Sampling and analytical methods

(1) Fourteen igneous rock samples were collected from different unit of the Habo alkaline intrusion. Among them, four were taken from Sandaoban unit, five from Habonanshan unit, three from Pingshan unit and two from Ashu unit. Those samples were, respectively, crushed to 60- to 80- mesh sizes and then 5.0 g pure feldspars were selected under a microscope. Those selected samples, then, were crushed to about 200-mesh size in an agate mortar. (2) 31 sulfur samples were collected from six deposits distributed around the Habo alkaline intrusion. Among them, 6 were collected from Habo Au deposit, 7 from Hageng Au deposit, 5 from Shapu Au deposit, 5 from Shee Pb deposit, 7 from Adong Pb–(Zn) deposit and 2 from Duojiao Pb–(Zn) deposit. Those samples were, respectively, crushed to 60- to 80- mesh sizes and then 5.0 g pure sulfur samples were selected under a microscope. After that, those selected samples were crushed to about 200-mesh size in an agate mortar and then were divided into two parts.

One part of the 31 sulfur samples was used to analyze sulfur isotope compositions at the State Key Laboratory of Environmental Geochemistry, Institute of Geochemistry, Chinese Academy of Sciences. The analytical instrument was a MAT252 gas mass spectrometer. The measured data are expressed by using international standard sulfur isotope CDT (Canyon Diablo Troilite) values and sulfur isotope standards GBW04414 (Ag_2S, $\delta^{34}S_{CDT} = -0.07$ ‰ ± 0.13 ‰) and GBW04415(Ag_2S, $\delta^{34}S_{CDT} = 22.15$ ‰ ± 0.14 ‰) as follows: $\delta^{34}S(‰) = [(^{34}S/^{32}S)_{sample}/(^{34}S/^{32}S)_{standard} - 1] \times 1000$. The analysis uncertainty was less than ±0.2 ‰ (2σ).

Fourteen igneous rock samples, along with the other part of the 31 sulfur samples, were sent to Wuhan Geological Survey Center, Chinese geological Survey to analyze Pb isotope compositions. The analytical instrument was a MAT-261 mass spectrometer. The measured ratio (2σ) of international standard sample is $^{207}Pb/^{206}Pb = 0.91455 \pm 0.00020$, and this is in accordance with the recommended value (0.91464 ± 0.00033).

4 Analytical results

4.1 S isotopic compositions

This study collected 31 sulfides, including pyrite, galena and sphalerite, from Au and Pb–(Zn) deposits. Test results are listed in Table 3, which indicates that those deposits have similar S isotopic compositions: (1) the $\delta^{34}S$ values of Au deposits range from −1.91 ‰ to 2.69 ‰ with Habo from −0.52 ‰ to 0.46 ‰ (mean value = −0.05 ‰), Hageng from −0.21 ‰ to 2.69 ‰(mean value = 1.13 ‰), and Shapu from −1.91 ‰ to 0.41 ‰ (mean value = −0.98 ‰); (2) the $\delta^{34}S$ values of Pb–(Zn) deposit range from −3.82 ‰ to 0.05 ‰ with Shee from −3.04 ‰ to −0.05 ‰ (mean value = −1.42 ‰), Adong from −3.82 ‰ to −0.47 ‰ (mean value = −2.72 ‰), and

Table 3 Sulfur isotopic compositions of pyrite, sphalerite and galena of Au and Pb–(Zn) deposits around the Habo alkaline intrusion

Ore deposit	Sample no.	Mineral	$\delta^{34}S$ (CDT ‰)	Mean (CDT ‰)	Ore deposit	Sample no.	Mineral	$\delta^{34}S$ (CDT ‰)	Mean (CDT ‰)
Habo Au deposit	HB0003	Pyrite	−0.32	−0.05	Hageng Au deposit	HG0003	Pyrite	0.05	1.13
	HB0005	Pyrite	0.01			HG0008	Pyrite	−0.21	
	HB0006	Pyrite	0.46			HG0027	Sphalerite	1.11	
	HB0007	Pyrite	0.05			HG0028	Pyrite	0.84	
	HB0012	Pyrite	0.05			HG0029	Pyrite	2.69	
	HB0014	Pyrite	−0.52			HG0030	Pyrite	2.32	
Shapu Au deposit	SP0010	Pyrite	−0.73	−0.98	Shee Pb deposit	SE0003	Pyrite	−3.04	
	SP0013	Pyrite	−0.41			SE0008	Pyrite	−2.11	
	SP0014	Pyrite	−0.53			SE0012	Pyrite	−1.81	−1.42
	SP0024	Pyrite	−1.91			SE0014	Pyrite	−0.08	
	SP0026	Pyrite	−1.32			SE0015	Pyrite	−0.05	
Adong Pb–(Zn) deposit	AD0007	Galena	−3.76	−2.72	Duojiao Pb–(Zn) deposit	DJ0006	Sphalerite	−3.37	
	AD0013	Galena	−3.44			DJ0012	Sphalerite	−3.45	−3.41
	AD0017	Sphalerite	−0.47						
	AD0018	Sphalerite	−3.82						
	AD0019	Sphalerite	−0.48						
	AD0022	Galena	−3.33						
	AD0024	Galena	−3.74						

Duojiao from −3.45 ‰ to −3.37 ‰ (mean value = −3.41 ‰).

4.2 Pb isotopic compositions

This study collected 14 feldspars from The Habo alkaline intrusion and 31 sulfides, including pyrite, galena and sphalerite, from Au and Pb–(Zn) deposits surrounding the Habo alkaline intrusion. Test results are listed in Table 4. The major findings are as follows. (1) Feldspar samples have relatively homogeneous isotopic compositions with $^{206}Pb/^{204}Pb$ ranging from 18.608 to 18.761, $^{207}Pb/^{204}Pb$ from 15.572 to 15.722 and $^{208}Pb/^{204}Pb$ from 38.599 to 39.110. μ values of feldspar samples range from 9.37 to 9.67 (mean value = 9.50). (2) The sulfide samples from Au deposits have relatively homogeneous isotopic compositions and they are, on the whole, similar to that of the alkaline intrusion feldspars within $^{206}Pb/^{204}Pb$ ranging from 18.564 to 18.734, $^{207}Pb/^{204}Pb$ from 15.582 to 15.738 and $^{208}Pb/^{204}Pb$ from 38.592 to 39.319. μ values of Au deposits ranging from 9.41 to 9.70 (mean value = 9.48). (3) The sulfide samples from Pb–(Zn) deposits show a decentralized trait, and most of them are similar to that of the alkaline intrusion feldspars within $^{206}Pb/^{204}Pb$ ranging from 18.523 to 18.648, $^{207}Pb/^{204}Pb$ from 15.599 to 15.802 and $^{208}Pb/^{204}Pb$ from 38.659 to 39.206. μ values of Pb–(Zn) deposits ranging from 9.44 to 9.84 (mean value = 9.64).

5 Discussions

5.1 The petrogenesis and tectonic setting

Previous work indicated that the most likely magma source mode of Ailaoshan-Red River Alkaline Rich Intrusive Rocks Belt is that in the process of paleotethys tectonic evolution, crust materials, which were brought in while formed the ancient subduction zone or ancient basement that came from ancient subduction slabs, and marine sediments were involved in the deep mixing action by recycle and formed the enriched mantle at the same time. After that, accompanied with the closure of neo-tethys and the consequent subduction and collision between India and Eurasia in latest cretaceous, the Tibetan plateau and its adjacent area (including western Yunnan area) lithosphere were significantly shortened and thickened. Magma source area, which was formed gradually and connected in the early Cenozoic, subjected partial melting when it rose up to crust-mantle mixing zone. Earlier studies have shown that Ailaoshan-Red River Alkaline Rich Intrusive Rocks are relatively rich in LILE (K, Rb, Ba and Sr, etc.) and loss in HFSE(Nb, Ta, P and Ti, etc.) and the ratios of La/Ce, Ce/Nd and Sm/Nd respectively range from 0.40 to 0.63, 1.88 to 2.81 and 0.11 to 0.20, which shows that the magma source has a crust-mantle mixing trait (Hou et al. 2007). As the biggest intrusion located in the south of the Ailaoshan-Red Rive fault system, the Habo porphyry intrusion and its surrounding deposits should have similar geology and

Table 4 Pb isotopic compositions of feldspars from the Habo alkaline intrusion and sulfides from Au and Pb–(Zn) deposits around the intrusion

Rock unit	Sample no.	Mineral	$^{206}Pb/^{204}Pb$	$^{207}Pb/^{204}Pb$	$^{208}Pb/^{204}Pb$	μ	Th/U	Δα	Δβ	Δγ
Sandaoban unit	ES0008	Feldspar	18.635	15.608	38.68	9.46	3.72	74.64	17.93	32.79
	ES0009	Feldspar	18.623	15.601	38.659	9.45	3.72	73.94	17.48	32.22
	ES0010	Feldspar	18.651	15.619	38.718	9.48	3.73	75.76	18.66	33.91
	ES0011	Feldspar	18.652	15.638	38.779	9.51	3.76	77.61	19.99	36.57
Habonanshan unit	EH0001	Feldspar	18.646	15.594	38.655	9.43	3.7	74.39	16.98	31.61
	EH0003	Feldspar	18.646	15.609	38.704	9.46	3.73	74.77	17.97	33.13
	EH0004	Feldspar	18.615	15.576	38.596	9.4	3.69	72.6	15.8	30.03
	EH0008	Feldspar	18.687	15.644	38.812	9.52	3.75	78.27	20.31	36.67
	EH0011	Feldspar	18.697	15.687	38.956	9.61	3.82	82.46	23.3	42.58
Pinshan unit	EP0001	Feldspar	18.7	15.646	38.842	9.53	3.76	78.49	20.42	37.17
	EP0003	Feldspar	18.71	15.692	38.983	9.61	3.82	82.98	23.62	43.17
	EP0005	Feldspar	18.761	15.722	39.11	9.67	3.85	86	25.58	46.61
Ashu unit	EA0005	Feldspar	18.663	15.618	38.724	9.47	3.73	75.68	18.56	33.63
	EA0007	Feldspar	18.704	15.677	38.929	9.59	3.8	81.51	22.58	41.09
Ore deposit										
Habo Au deposit	HB0003	Pyrite	18.641	15.613	38.719	9.47	3.73	75.15	18.27	33.92
	HB0005	Pyrite	18.621	15.602	38.681	9.45	3.73	74.04	17.55	32.93
	HB0006	Pyrite	18.62	15.588	38.643	9.42	3.71	72.89	16.59	31.29
	HB0007	Pyrite	18.628	15.593	38.655	9.43	3.71	73.35	16.91	31.61
	HB0012	Pyrite	18.635	15.594	38.658	9.43	3.71	73.75	16.98	31.69
	HB0014	Pyrite	18.663	15.62	38.761	9.48	3.74	75.88	18.7	34.73
Hageng Au deposit	HG0008	Pyrite	18.625	15.632	38.753	9.61	3.76	76.97	19.65	36.39
	HG0027	Sphalerite	18.564	15.63	38.682	9.51	3.76	76.65	19.68	36.33
	HG0028	Pyrite	18.618	15.584	38.599	9.41	3.69	72.77	16.33	30.11
	HG0029	Pyrite	18.603	15.587	38.607	9.42	3.7	72.53	16.55	30.68
	HG0030	Pyrite	18.6	15.582	38.592	9.41	3.7	72.03	16.21	30.1
	HG0035	Pyrite	18.588	15.602	38.628	9.45	3.72	73.97	17.65	32.56
Shapu Au deposit	SP0010	Pyrite	18.71	15.69	38.983	9.61	3.82	82.78	23.48	43.06
	SP0013	Pyrite	18.647	15.654	38.827	9.55	3.78	79.15	21.13	38.89
	SP0014	Pyrite	18.734	15.738	39.319	9.7	3.88	87.48	26.78	53.94
	SP0026	Pyrite	18.672	15.663	38.87	9.56	3.79	80.08	21.69	39.75
Shee Pb deposit	SE0003	Pyrite	18.644	15.705	38.919	9.65	3.83	84.12	24.73	44.28
	SE0008	Pyrite	18.648	15.731	39.015	9.7	3.87	86.62	26.55	48.13
	SE0012	Pyrite	18.599	15.599	38.659	9.44	3.73	73.7	17.4	32.87
	SE0014	Pyrite	18.624	15.606	38.684	9.45	3.73	74.43	17.83	33.13
	SE0015	Pyrite	18.603	15.599	38.659	9.44	3.73	73.7	17.39	32.74
Adong Pb–(Zn) deposit	AD0007	Galena	18.58	15.756	39.028	9.75	3.92	88.83	28.54	51.95
	AD0013	Galena	18.604	15.802	39.206	9.84	3.99	93.3	31.72	58.46
	AD0017	Sphalerite	18.549	15.726	38.917	9.7	3.88	85.9	26.51	48.34
	AD0018	Sphalerite	18.529	15.708	38.847	9.66	3.86	84.09	25.3	46.1
	AD0022	Galena	18.549	15.72	38.899	9.68	3.87	85.34	26.09	47.54
	AD0024	Galena	18.53	15.715	38.883	9.68	3.88	84.78	25.79	47.42
Duojiao Pb–(Zn) deposit	DJ0006	Sphalerite	18.523	15.713	38.878	9.67	3.88	84.61	25.68	47.42
	DJ0012	Sphalerite	18.528	15.713	38.873	9.67	3.87	84.59	25.66	47.11

geochemistry characteristics with those in the middle and north of the tectonic belt. Studies have shown that in the Ailaoshan-Red Rive fault system, except the fact that the mineralization of Mojiang gold deposit has a deep relation with ultrabasic rocks, almost all of the mineralization of gold deposits have deep space and genesis relations with

the Himalayan alkali rich porphyry (Bi and Hu 1998). The porphyry that have close relations with Au mineralization are a rock series ranging from basic to intermediate-acidic and show a alkali-rich with $K_2O + Na_2O > 8$ %. Those rocks, including Monzonite granite porphyry, Monzonite porphyry and a little Syenite porphyry, are occurred as the veins and shows a composite rock mass trait. In the rock mass, mineralization has a close relation with acidic porphyry that invaded in mid-late and the mineralization occurs at 3–1 Ma before the invasion of last ore-forming porphyry (Hou et al. 2003). Rock types, from north to south, changed from Monzonitic granite porphyry to Syenite porphyry. Most of Alkali rich rocks occurred in this area at about 50–20 Ma and concentrated in time of 38–33 Ma, which is consistent with the time when mass Au-rich mineralization happened in this area (Wang et al. 2004). Our unpublished data, recently, has indicated that the Habo alkali rocks invaded at time 36–33 Ma, and the Habo porphyry intrusion shows a trait of Arc magma and its magma source mode is crust-mantle, which is in accordance with studies on regional. In conclusion, it can be seen from rock series, magma source and petrogenic age that the Habo alkaline intrusion is part of Ailaoshan-Red River Alkaline Rich Intrusive Rocks Belt and they should share the same mineralization geotectonic setting.

5.2 The source of ore-forming elements

5.2.1 Sulfur

The fractionation of sulfur isotopes widely exists in nature, so the sulfur isotopes are widely used to trace the source of ore-forming materials, and then the genesis of ore deposits can be discussed (Ohmoto 1986). Studies have shown that there are three isotopically distinct reservoirs of $\delta^{34}S$: (1) mantle-derived sulfur with $\delta^{34}S$ values in the range 0 ± 3 ‰ (Chaussidon and Lorand 1990); (2) seawater sulfur with $\delta^{34}S$ today about +20 ‰, although this value has varied in the past, and (3) strongly reduced (sedimentary) sulfur with large negative $\delta^{34}S$ values.

It can be seen from the sulfur isotopic data that almost all of the $\delta^{34}S$ values range from −4.0 ‰ to 4.0 ‰, which indicates, combined with the sulfur isotopes diagram (Fig. 5), ore-forming elements mainly derived from magmatic fluids. This is consistent with the Beiya area (Li et al. 2001; Zhou et al. 2016), which was typically a porphyry Au polymetallic deposits located in the north of the Habo alkaline intrusion. Most importantly, the decreasing trend of $\delta^{34}S$ values among those deposits (Table 3) is as follows: 1.13 ‰ to −0.05 ‰ to −0.98 ‰ to −1.42 ‰ to −2.72 ‰ to −3.41 ‰, which may indicate that the source of ore-forming elements of Au and Pb–(Zn) deposits derived from the Habo alkaline intrusion, the fractionation effects of sulfur isotopes may lead to the decreasing trend happened during hydrothermal migration and ore formation process.

5.2.2 Metal elements

Pb isotopic compositions will not change so much except physical, chemical and biological processes caused by radioactive decay and maintain relative stability during ore-forming elements migration and precipitation, making Pb isotopic compositions a direct way to trace the source of ore-forming materials (e.g. Zhu 1995; Canals and Cardellach 1997). It is of an important way to trace the source of ore-forming materials by comparing the Pb isotopic compositions of ores, magmas and basement rocks (e.g. Zhang et al. 2000; Wu et al. 2004). Research indicates that radioactive Pb of sulfide ores can be neglected because it contains lower U and Th elements. Magmatic feldspars Pb isotopic compositions, however, can approximately represent the Pb isotopic compositions of magmas and ores, and Pb isotopic compositions should be similar to that of magmas if ores come from magmatic differentiation (e.g. Zhang et al. 2000).

Data listed in Table 4 shows that the Habo alkaline intrusion, Habo Au deposit, Hageng Au deposit, Shapu Au deposit, Shee Pb deposit, Adong Pb–(Zn) deposit and Duojiao Pb–(Zn) deposit almost share the same Pb isotopic compositions, and the source materials of the Habo alkaline intrusion, Au, and Pb–(Zn) deposits belong to the crust-mantle mixed type, which are similar to that of Beiya (Li 2009; Kan 2013; Zhou et al. 2016). In the plumbotectonic diagram (Fig. 6), the Pb isotopic compositions of the Habo alkaline intrusion, Au, and Pb–(Zn) deposits are mainly located near the area of orogenic belt growth curve (Zartman and Doe 1981) and almost all of Au and Pb–(Zn) deposits have the same projection area with the Habo alkaline intrusion except that some samples of Adong Pb–(Zn) deposit slightly deviate from this area, which indicates that these Au and Pb–(Zn) deposits almost share the same source materials with the Habo alkaline intrusion. Besides, (1) the Th/U values of feldspars are slightly higher than that of the mantle in mainland China (mean value = 3.60, Zheng and Zhou 2001) and are obviously lower than that of the lower crust of China (mean value = 5.48, Zheng and Zhou 2001) with ranging from 3.68 to 3.85 (mean value = 3.74), which suggests that the source materials of The Habo alkaline intrusion, whose feldspars characterized by lower μ values and Th/U values, belong to the crust-mantle mixed type. (2) The Th/U values of sulfides from Au deposits are almost similar to that of the Habo alkaline intrusion feldspars with Th/U values ranging from 3.69 to 3.88 (mean value = 3.77). 3) The Th/U

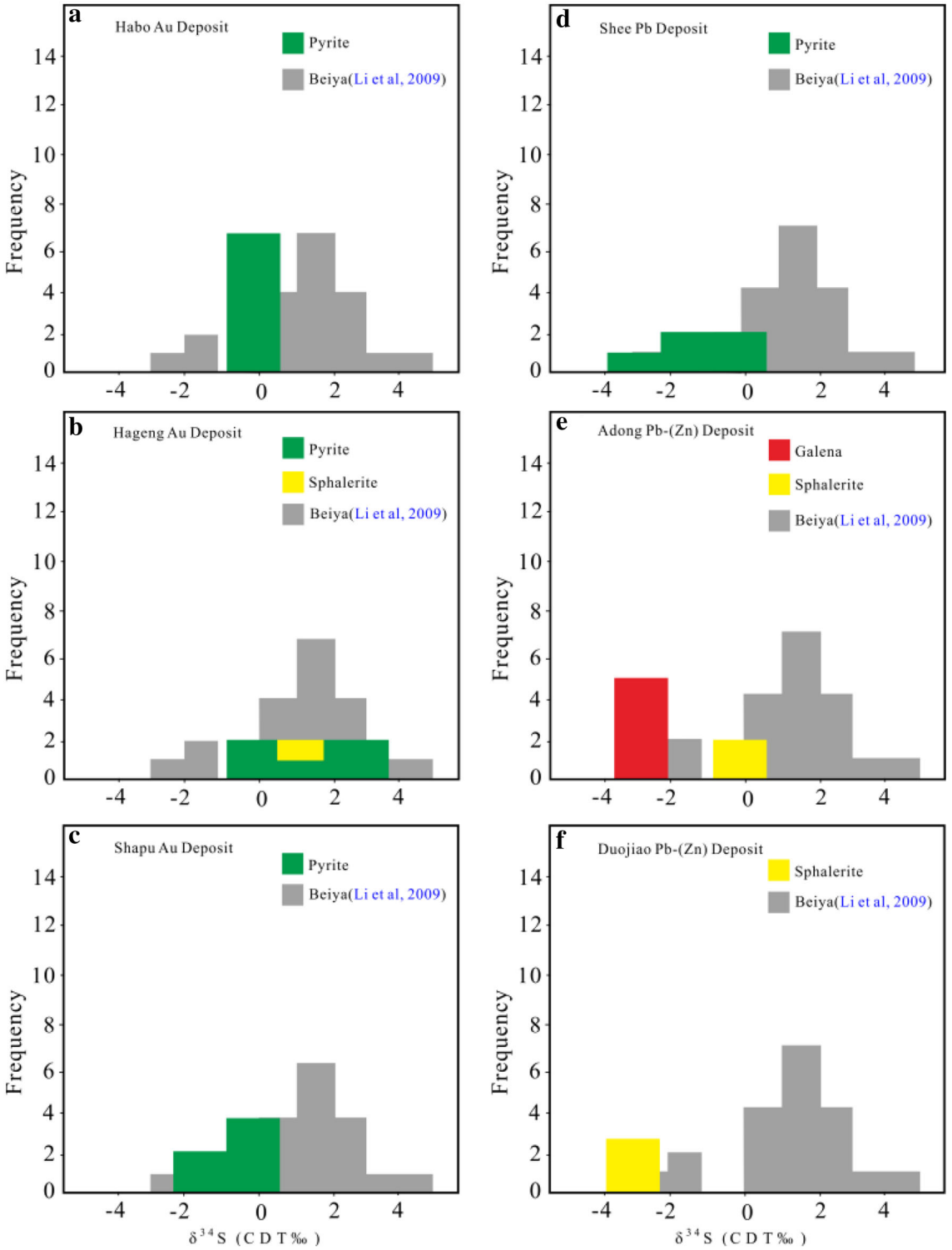

Fig. 5 Histograms of sulfur isotopes of Au and Pb–(Zn) deposits around the Habo alkaline intrusion

values of sulfides from Pb–(Zn) deposits are slightly higher than that of the Habo alkaline intrusion feldspars with Th/U values ranging from 3.73 to 3.99 (mean value = 3.84). It can be seen that the Th/U values of these deposits are slightly higher than that of the mantle of mainland China and are obviously lower than that of the lower crust of China.

Otherwise, a large number of ore and rock Pb isotopic compositions of stduies show that the changes of Th–Pb and the mutual relationships between Th–Pb and U–Pb

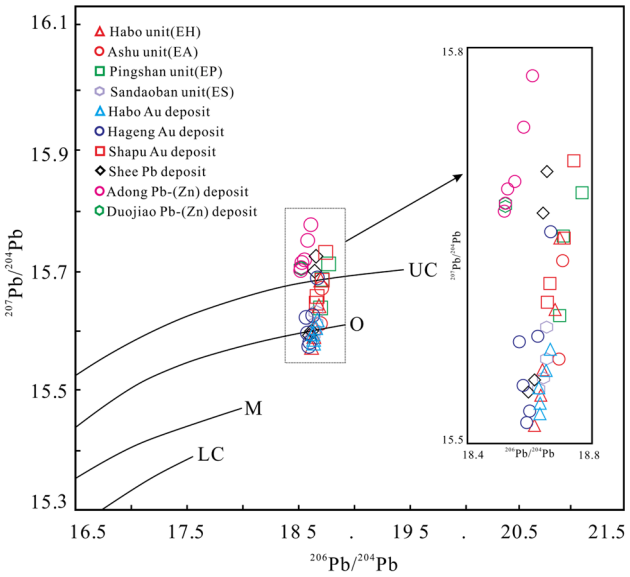

Fig. 6 Plot of $^{207}Pb/^{204}Pb$ versus $^{206}Pb/^{204}Pb$ for Habo alkaline intrusion and its surrounding Au and Pb–(Zn) deposits (Based on Zartman and Doe 1981). *LC* lower crust, *M* mantle, *O* orogene, *UC* upper crust

isotopic compositions can provide abundant information for geological process and source material. For the sake of highlighting the changing relationship between Pb isotopic compositions and eliminating the impact of time, we can describe three Pb isotopic compositions as relative deviations (Δα, Δβ and Δγ) between three Pb isotopic compositions and contemporary mantle Pb isotopic compositions and put forward the Δγ−Δβ genetic diagram of ore Pb isotopic compositions (Zhu 1998). We calculate relative deviations of Pb isotopic compositions of monominerals (feldspar and sulfides) and contemporary mantle Pb isotopic compositions (Table 4), and then project those data on Δγ−Δβ genetic diagram (Fig. 7). It, firstly, can be seen that almost all of the data from the four rock units of Habo porphyry intrusion are located in the magmatism area (Fig. 7a) except some samples from Pinshan unit. Secondly, almost all of the projection points of Au deposits are located in the magmatism area (Fig. 7b), except part samples of Shapu slightly deviate from the magmatism area. Finally, almost all of the projection points of Pb–(Zn) deposits are located in the upper crust area (Fig. 7b), except part samples of Shee are located in the magmatism area. It can be seen that the Au deposits almost share the same projection area, and this means that both of them share the same source materials. However, the continual linear distribution of the projection points, Au to Pb–(Zn) deposits, from magmatism to upper crust area (Fig. 7b) may suggest that the Pb–(Zn) deposits share the same source ore-forming elements with Au deposits, and parts of sedimentary materials involved in during hydrothermal migrations and ore formation process.

It may be wise to conclude from the sulfur and Pb isotopic composition data (Tables 3, 4) and diagrams (Figs. 5, 6, 7) that all of deposits almost share the same source materials with the Habo alkaline intrusion, and the source

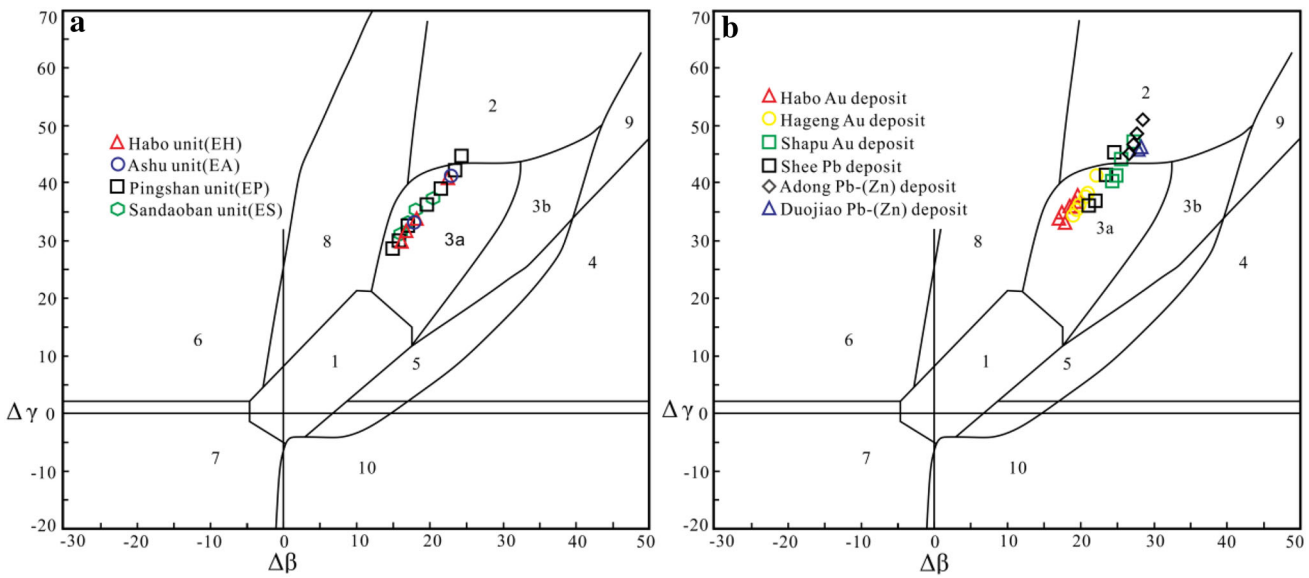

Fig. 7 The Pb isotope Δγ−Δβ genetic diagrams of Habo alkaline intrusion and its surrounding Au and Pb–(Zn) deposits (based on Zhu et al. 1998). (*1*) Mantle source area, (*2*) Upper crust source area, (*3*) The Subduction zone source area; (*3a*). Magmatism; (*3b*). Sedimentation, (*4*) Chemical deposition source area, (*5*) Submarine hydrothermal deposition source area, (*6*) Mid-level metamorphism source area, (*7*). Hypozonal metamorphism lower crust source area; (*8*) Orogene source area, (*9*) Old upper crust shale source area, (*10*) Regressive metamorphism source area

differences between some deposits, like Adong Pb deposit and Duojiao Pb deposit, and the Habo alkaline intrusion maybe some sedimentary materials involved in during hydrothermal migrations and ore formation process. It is, however, very hard but most important to distinguish what rock unit of this alkaline intrusion contributes the source materials with certain deposit so that it can guide prospecting, and this needs more researches in the future.

5.3 Ore genesis and metallogenic series

Metallogenic series mainly study relations among deposits from the angle of deposit types. Cheng et al. (1979, 1983) suggested that metallogenic series is a natural association of deposits, which included different minerals and types of deposits that formed in different metallogenic stages and geological structures, which genetically related with certain geological metallogenesis in certain geological tectonic unit and geological time. Zhai and Xiong (1987) emphasized relations between ore genesis and rock structure and proposed that metallogenic series is four-dimensional geological body that formed by a series of type deposits that genetically related with the same rock structure. Chen (1994) indicated that in order to better conduct comparison study among different deposits and understand common features and metallogenic rule of those deposits, it is reasonable to category those who share similar geological environment, metallogenic feature, and association of deposits as a metallogenic series though they formed in different geological time and unit. Chen (1997) further pointed out metallogeic series is a natural geological body, which was composed by a series genetically related deposits.

The Habo ore field is a Cu, Mo, Fe, Au, Pb, and Zn polymetallic ore accumulated area and its ore genesis types are relatively complex. Though the differences of ore-controlling structures, occurrence positions, attitudes and scales, those deposits show a characteristic centered by the Habo alkaline intrusion, inside-out, formed a series of associations of deposits, which concretely showed as follows: (1) porphyry Cu–Mo deposits within the intrusion; (2) hydrothermal vein type Fe–Au deposits occurred in the exocontact fault structure zone and wall rock crack; (3) hydrothermal vein type Pb–(Zn) deposits occurred in the fault structure zone and wall rock crack away from the intrusion. Ore-forming materials studies showed that the source ore-forming elements of Cu–Mo (Zhu et al. 2013), Au and Pb–(Zn) deposits are similar to that of the Habo alkaline intrusion. We, hence, suggest that the Cu–Mo, Au and Pb–(Zn) deposits in the Habo ore filed belong to a porphyry metallogenic series. This series includes porphyry Cu–Mo, magma-related fracture hydrothermal vein type Fe–Au, and magma-related fracture hydrothermal vein type Pb–(Zn) deposits. Otherwise, isotopic age of the Habo alkaline intrusion is 36–33 Ma (Zhu et al. 2013; our unpublished data), which is similar to that of Beiya (a typical Cenozoicalkaline porphyries deposit in the Ailaoshan-Red River Cenozoic Ore System), whose ore-related alkaline porphyries age is 38–31 Ma and molybdenite Re–Os age is 36.9 Ma (Zhou et al. 2016; He et al. 2013). Therefore, along with S–Pb isotope traits, we suggest that the Habo Au and Pb–(Zn) deposits are typically Ailaoshan-Red RiverCenozoicalkaline-related deposits and ore-forming ages of these deposits are later than that of the Habo alkaline intrusion.

6 Conclusions

(1) S–Pb isotopic data suggest that the Habo alkaline intrusion and Au and Pb–(Zn) deposits around it are genetically linked.
(2) The Habo Cu–Mo, Au, and Pb–(Zn) deposits belong to a porphyry metallogenic series. This series includes porphyry Cu–Mo, magma-related fracture hydrothermal vein type Fe–Au, and magma-related fracture hydrothermal vein type Pb–(Zn) deposits.
(3) The Habo Au and Pb–(Zn) deposits are typically Ailaoshan-Red River Cenozoicalkaline-related deposits and ore-forming ages of these deposits are later than that of the Habo alkaline intrusion.

Acknowledgments This study thanks Yunnan No. 2 Geological Survey for providing plenty of field data. We are also grateful to State Key Laboratory of Environmental Geochemistry, Institute of Geochemistry, Chinese Academy of Sciences and Wuhan Geological Survey Center, Chinese geological Survey for providing technical supports on isotopic analysis.

Compliance with ethical standards

Conflict of interest There is no Conflict of interest.

References

Basuki NI, Taylor BE, Spooner ETC (2008) Sulfur isotope evidence for thermochemical reduction of dissolved sulfate in Mississippi valley type zinc—lead mineralization, Bongara area, northern Peru. Econ Geol 103:183–799

Bi XW, Hu RZ (1998) REE geochemistry of ore-forming fluids from Ailaoshan gold metallogenic belt. Geol Rev 44(3):48–87 **(in Chinese with English abstract)**

Bi XW, Hu RZ, Peng JT (2005) The geochemistry traits of alkaline-rich porphyry intrusions from Yaoan and Machangqing. Acta Pet Sin 21(1):113–124 **(in Chinese with English abstract)**

Canals A, Cardellach E (1997) Ore lead and sulphur isotope patternfrom the low-temperature veins of the Calalonian Coastal Ranges (NE Spain). Miner Depos 32:243–249

Chaussidon M, Lorand JP (1990) Sulfur isotope composition of orogenic spinel lherzolite massifs from Ariege (North-Eastern

Pyrenees, France): an ion microprobe study. Geochim Cosmochim Acta 54(10):2835–2846
Chen YC (1994) Metallogenic series of ore deposits. Earth Sci Front 1(3–4):105–118 **(in Chinese with English abstract)**
Chen YC (1997) Present situation and trend of research on metallogenic series of ore deposits. Geol Prospect 33(1):21–25 **(in Chinese with English abstract)**
Cheng YQ, Chen YC, Zhao YM (1979) Preliminary discussion on the problems of minerogenetic series of mineral deposits. Bull Chin Acad Geol Sci 1(1):32–58 **(in Chinese with English abstract)**
Cheng YQ, Chen YC, Zhao YM, Song TR (1983) Further discussion on the problems of minerogenetic series of mineral deposits. Bull Chin Acad Geol Sci 6:1–64 **(in Chinese with English abstract)**
Chung SL, Lee TY, Lo CH et al (1997) Intraplate extension prior to continental extrusion along the Ailaoshan-Red River shear zone. Geology 25:311–314
He WX, Mo XX, Yu XH, He ZH et al (2013) Zircon U–Pb and Molybdenite Re–Os dating for the Beiya Au polymetallic deposit in the western Yunnan Province and its geological significance. Acta Pet Sin 29:1301–1310 **(in Chinese with English abstract)**
Hou ZQ, Ma HW, Khin Z, Zhang YQ (2003) The Himalayan Yulong porphyry copper belt: produced by largescale strike- slip faulting at Eastern Tibet. Econ Geol 98:125–145
Hou ZQ, Pan GT, Wang AJ (2006) Qinghai-Tibet plateau collision orogen: late II collision conversion mineralization. Miner Depos 25(5):521–543 **(in Chinese with English abstract)**
Hou ZQ, Zaw K, Pan GT, Mo XX, Xu Q, Hu YZ, Li XZ (2007) The Sanjiang Tethyan metallogenesis in S.W.China: tectonic setting, metallogenic epoch and deposit type. Ore Geol Rev 31(1–4):48–87
Hu RZ, Burnard PG, Bi XW (2004) Helium and argon isotope geochemistry of alkaline intrusion-as sociated gold and copper deposits along the Red River-Jinshajiang fault belt, SW China. Chem Geol 203:305–317
Ji JQ, Zhong DL, Zhang LS (2000) Kinematics and dating of Cenozoic strike-slip faults in the Tengchong area, west Yunnan: implications for the block movement in the southeastern Tibet Plateau. Chin J Geol 35(3):336–349
Kan YS (2013) Geological and geochemical characteristics of Beiya gold deposits. Dissertation, China University of Geosciences, Beijing (in Chinese with English abstract)
Li Y (2009) The metallogenic geochemistry and significance of Prospecting of gold polymetallic ore concentration area in Beiya in western Yunnan Province. Dissertation, China University of Geosciences, Beijing **(in Chinese with English abstract)**
Li L, Zheng YF, Zhou JB (2001) The lead isotope evolution model of Chinese mainland. Acta Petrol Sin 17(1):61–68 **(in Chinese with English abstract)**
Ohmoto H (1972) Systematics of sulfur and carbon isotopes in hydrothermal ore deposits. Econ Geol 67:551–579
Ohmoto H (1986) Stable isotope geochemistry of ore deposits. Rev Mineral 6:491–559
Ohmoto H, Kaiser CJ, Geer KA (1990) Systematics of sulphur isotopes in recent marine sediments and ancient sediment-hosted base metal deposits. In: Herbert HK, Ho SE (eds) Stable isotopes and Fluid Processes in Mineralization. Geology Department & University Extension, The University of Western Australia, Perth, pp 70–120
Rey RO, Sawkins FJ (1974) Fluid inclusion and stable isotope studies on Casapalca Ag–Pb–Zn–Cu deposit, Central-Andes. Peru Econ Geol 69(2):181–205
Seal RR (2006) Sulfur isotope geochemistry of sulfide minerals. R Miner Geochem 61:633–677
Turner S, Arnaud N, Liu JQ (1996) Post- collision, shoshonitic volcanism on the Tibetan plateau: implications for convective thinning of the lithosphere and the source of ocean island basalts. J Pet 37:45–71
Wang EQ, Burchfiel BC (1997) Interpretation of Cenozoic tectonics in the right-lateral accommodation zone between the Ailaoshan shear zone and the eastern Himalayan syntaxis. Int Geo Rev 39:191–219
Wang JH, Yin A, Harrison TM (2001) A tectonic model for Cenozoic igneous activities in the eastern Indo-Asian collision zone. Earth Planet Sci Lett 188:123–133
Wang DH, Qu WJ, Li ZW (2004) The principal metallogenic epoch of Porphyry Cu–Mo deposits from Jing Sha River-Red River metallogenic belt: Re–Os isotope dating. Sci China (Ser D) 34(4):345–349 **(in Chinese with English abstract)**
Wu KH, Hu RZ, Bi XW, Zhang Q, Peng JT (2004) The explaining of upper mantle lead isotope evolution model and lead isotope compositions from alkaline porphyry of western Yunnan. China. Acta Geosci Sin 25(2):263–270 **(in Chinese with English abstract)**
Yin A, Harrison TM (2000) Geologic evolution of the Himalayan-Tibetan orogen. J Ann Rev Earth Planet Sci 28:211–280
Zartman RE, Doe BR (1981) Plumbotectonics-the model. Tectonophysics 75:135–162
Zhai YS, Xiong YL (1987) On the structure of the metallogenic series. Earth Sci J Wuhan Coll Geol 12(4):375–380 **(in Chinese with English abstract)**
Zhang YQ, Xie YW (1997) The geochronology and characteristics of Nd, Sm isotope of Aailaoshan-Jingshajiang alkali-rich intrusive rocks. Sci China (Ser D) 27(4):289–293
Zhang YQ, Xie YW, Tu GZ (1987) A preliminary study on the relations between Ailaoshan-Jinshajiang River alkaline-rich intrusion and fault structures. Acta Pet Sin 3(1):17–25 **(in Chinese with English abstract)**
Zhang Q, Pan JY, Shao SX (2000) An interpretation of ore sources from lead isotopic compositions of some ore deposits in China. Geochimica 29(3):231–238 **(in Chinese with English abstract)**
Zhang B, Zhang JJ, Zhong DL (2009) Strain and kinematic vorticity analysis: an indicator for sinistral transpressional strain-partitioning along the Lancangjiang shear zone, western Yunnan China. Sci China 52(5):602–618
Zhao DK, Wang HS, Xue HY (2009) Analysis of the geology traits and genetics of the Habo Cu–Mo–Au deposit, Yunna Chinan. Acta Geol Sin 33(3):230–234 **(in Chinese with English abstract)**
Zheng YF, Hoefs JC (1993) Effects of mineral precipitation on the sulfur isotope composition of hydrothermal solutions. Chem Geol 105(4):259–269
Zhou JX, Huang ZL, Zhou GF, Jin ZG, Li XB, Ding W, Gu J (2010) Sources of the ore metals of the Tianqiao Pb–Zn deposit in Northwestern Guizhou Province: constraints form S, Pb isotope and REE Geochemistry. Geol Rev 56(4):513–524 **(in Chinese with English abstract)**
Zhou JX, Huang ZL, Bao GP (2013a) Geological and sulfur-lead-strontium isotopic studies of the Shaojiwan Pb–Zn deposit, southwest China: implications for the origin of hydrothermal fluids. J Geochem Explor 128:51–61
Zhou JX, Huang ZL, Yan ZF (2013b) The origin of the Maozu carbonate-hosted Pb–Zn deposit, southwest China: constrained by C–O–S–Pb isotopic compositions and Sm–Nd isotopic age. J Asian Earth Sci 73:39–47
Zhou JX, Huang ZL, Zhou MF, Zhu XK, Muchez P (2014) Zinc, Sulfur, and lead isotopic variations in carbonate-hosted Pb–Zn sulfide deposits, southwest China. Ore Geol Rev 58:41–54
Zhou JX, Huang ZL, Dou S, Cui YL, Ye L, Li B, Gan T, Sun HR (2016) Origin of the Luping Pb deposit in the Beiya area, Yunnan Province, SW China: constraints from geology, isotope geochemistry. Ore Geol Rev 72:179–190

Zhu BQ (1995) The mapping of geochemical provinces in China based on Pb isotopes. J Geochem Explor 55:171–181

Zhu BQ (1998) Concurrently discussed the crust-mantle evolution of Chinese continental. In: Coleman RG, Wang XM (eds) Theories and applications of isotopic system in geosciences. Science Press, Beijing, p 221

Zhu XP, Mo XX, White NC (2009) Research of ore geology and ore-forming background from the Habo Cu–Mo–Au deposit, Yunnan China. Acta Geol Sin 83(12):1915–1928 **(in Chinese with English abstract)**

Zhu XP, Mo XX, White NC, Zhang B, Sun MX, Wang SX, Zhao Y (2013) Petrogenesis and metallogenic setting of the Habo porphyry Cu–(Mo–Au) deposit. Yunnan, China. J Asian Earth Sci 66:188–203